Single Crystal X-ray Diffraction Study of the Spinel-type LiMn$_2$O$_4$

Junji Akimoto,* Yasuhiko Takahashi, Yoshito Gotoh, and Susumu Mizuta

National Institute of Materials and Chemical Research,1-1 Higashi, Tsukuba, 305-8565, Japan

Lithium manganese oxide, LiMn$_2$O$_4$, is an attractive cathode material for lithium ion rechargeable batteries owing to its cost and environmental performance.[1] Recently, much attention has been paid to the structural and physical properties of this compound, investigated by various techniques such as NMR,[2] XAFS,[3,4] magnetism,[5,6] and diffraction techniques.[7–10] The stoichiometric compound LiMn$_2$O$_4$ presents a first-order structural transition around room temperature. Above the transition temperature it has the cubic spinel structure with $Fd\bar{3}m$ space group.[11] The crystal structure of the low temperature form has been investigated at 280, 230, and 100 K using the neutron and synchrotron radiation X-ray powder diffraction method. Rousse and co-workers[12–14] and Massarotti et al.[15] reported an orthorhombic $\sim 3a \times 3a \times a$ superstructure of the basic cubic spinel structure, while Wills et al. refined using a tetragonal $\sim 2a \times 2a \times a$ superstructure model.[6]

To clarify the true crystal symmetry, precise crystal structure, the mechanism of the structural transition, and physical properties of LiMn$_2$O$_4$, sizable, well-characterized single crystal specimens have highly been desired, as in the study of Fe$_3$O$_4$ magnetite,[16] though corresponding single crystals with good quality have not yet been synthesized. In the present study, we report the single crystal synthesis and the X-ray structure
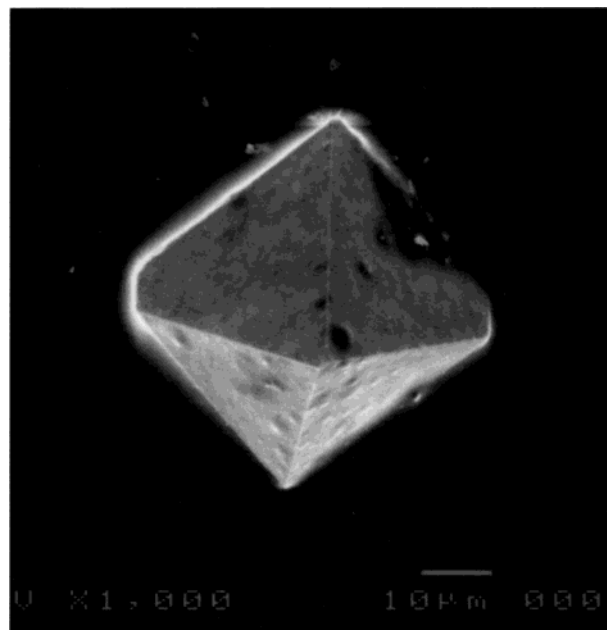

Figure 1. SEM photograph of single crystal of LiMn$_2$O$_4$.

refinement of the first single crystal of the spinel-type LiMn$_2$O$_4$. We will also demonstrate the structural phase transition around room temperature by single-crystal X-ray diffraction method.

Starting materials for the crystal growth were the as-prepared LiMn$_2$O$_4$ powder (Cell Seed M, Nippon Chemical Industrial Co., Ltd., Tsukuba, Japan) and lithium chloride powder (99.9%). These materials were well-mixed in the nominal weight ratio of LiMn$_2$O$_4$:LiCl = 1:8, sealed in a gold tube, heated at 1173 K for 10 days, and gradually cooled to 297 K at a rate of 5 K/h. The produced single crystals were easily separated from the frozen flux materials by rinsing the gold tube in water for several minutes.

Black, octahedral-shape single crystals of about 0.05 × 0.05 × 0.05 mm^3 in maximum were obtained, as shown in Figure 1. SEM–EDX analysis showed that the crystals were free from gold contamination from the tube. The chemical formula, analyzed by inductive coupled plasma spectroscopy (ICP) using the pulverized crystals, confirmed the stoichiometric chemical composition; the result was consistent with that of the present structure refinement. X-ray precession photographs taken at 298 K using Mo Kα radiation indicate that the crystals belong to the cubic spinel structure with $Fd\bar{3}m$ space group.

The spinel structure was carefully investigated at 297 K by single-crystal X-ray diffraction method. The intensity data were collected by the $2\theta-\omega$ scan mode with a scan rate of 1°/min at 297 K on a four-circle diffractometer (Rigaku AFC-7R, operating conditions: 50 kV, 180 mA) using graphite-monochromatized Mo Kα radiation ($\lambda = 0.710\ 73$ Å). A summary of the crystallographic and experimental data is given in Table 1. All calculations were carried out using the XTAL3.4 program.[17] The refined lattice parameter and the oxygen parameter x are in good agreement with the previous results for the stoichiometric LiMn$_2$O$_4$ using neutron powder dif-

* Corresponding author. E-mail: akimoto@nimc.go.jp. Fax: +81-298-61-4555.

(1) Thackeray, M. M. *Prog. Solid State Chem.* **1997**, *25*, 1.
(2) Shiraishi, Y.; Nakai, I.; Tsubata, T.; Himeda, T.; Nishikawa, F. *J. Solid State Chem.* **1997**, *133*, 587.
(3) Yamaguchi, H.; Yamada, A.; Uwe, H. *Phys. Rev. B* **1998**, *58*, 8.
(4) Lee, Y. J.; Wang, F.; Grey, C. P. *J. Am. Chem. Soc.* **1998**, *120*, 12601.
(5) Shimakawa, Y.; Numata, T.; Tabuchi, J. *J. Solid State Chem.* **1997**, *131*, 138.
(6) Wills, A. S.; Raju, N. P.; Greedan, J. E. *Chem. Mater.* **1999**, *11*, 1510.
(7) Sugiyama, J.; Atsumi, T.; Koiwai, A.; Sasaki, T.; Hioki, T.; Noda, S.; Kamegashira, N. *J. Phys.: Condens. Matter.* **1997**, *9*, 1729.
(8) Yamada, A.; Tanaka, M. *Mater. Res. Bull.* **1995**, *30*, 715.
(9) Oikawa, K.; Kamiyama, T.; Izumi F.; Chakoumakos, B. C.; Ikuta, H.; Wakihara M.; Li, J.; Matsui, Y. *Solid State Ionics* **1998**, *109*, 35.
(10) Hayakawa, H.; Takada, T.; Enoki, H.; Akiba, E. *J. Mater. Sci. Lett.* **1998**, *17*, 811.
(11) Strobel, P.; Le Cras, F.; Seguin, L.; Anne, M.; Tarascon, J. M. *J. Solid State Chem.* **1998**, *135*, 132.
(12) Rousse, G.; Masquelier, C.; Rodríguez-Carvajal, J.; Hervieu, M. *Electrochem. Solid-State Lett.* **1999**, *2*, 6.
(13) Rodríguez-Carvajal, J.; Rousse, G.; Masquelier, C.; Hervieu, M. *Phys. Rev. Lett.* **1998**, *81*, 4660.
(14) Rousse, G.; Masquelier, C.; Rodríguez-Carvajal, J.; Elkaim, E.; Lauriat, J.-P.; Martínez, J. L. *Chem. Mater.* **1999**, *11*, 3629.
(15) Massarotti, V.; Capsoni, D.; Bini, M.; Scardi, P.; Leoni, M.; Baron, V.; Berg, H. *J. Appl. Crystallogr.* **1999**, *32*, 1186.
(16) Iizumi, M.; Koetzle, T. F.; Shirane, G.; Chikazumi, S.; Matsui, M.; Toda, S. *Acta Crystallogr. B* **1982**, *38*, 2121.
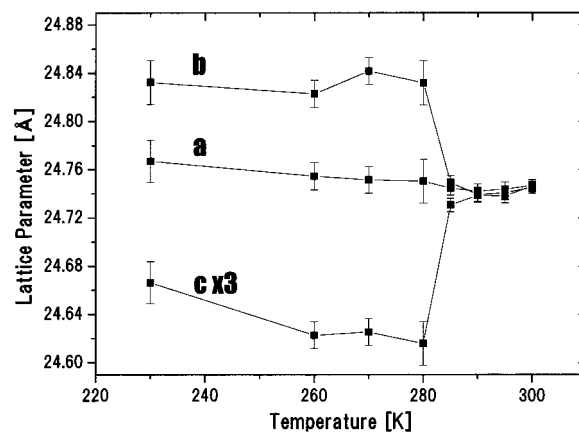
Table 1. Crystallographic and Experimental Data for LiMn$_2$O$_4$ at 297 K

structural formula	LiMn$_2$O$_4$
cryst system	cubic
space group	$Fd\bar{3}m$
a (Å)	8.2483(6)
V (Å^3)	561.16(13)
cryst size (μm)	30 × 30 × 30
max 2θ (deg)	90
abs cor method	Gaussian integration
no. of measd reflcns	2037
no. of obsd reflcns ($>5\sigma$)	82
no. of variables	7
R	0.024
wR [$w = 1/\sigma^2 F$]	0.017
U_{eq} for Li at ($^1/_8$, $^1/_8$, $^1/_8$)	0.010(2)
U_{eq} for Mn at ($^1/_2$, $^1/_2$, $^1/_2$)	0.00928(16)
x for O at (x, x, x)	0.26320(18)
U_{eq} for O at (x, x, x)	0.0171(5)
Li−O (×4) distance (Å)	1.9744(15)
Mn−O (×6) distance (Å)	1.9592(15)
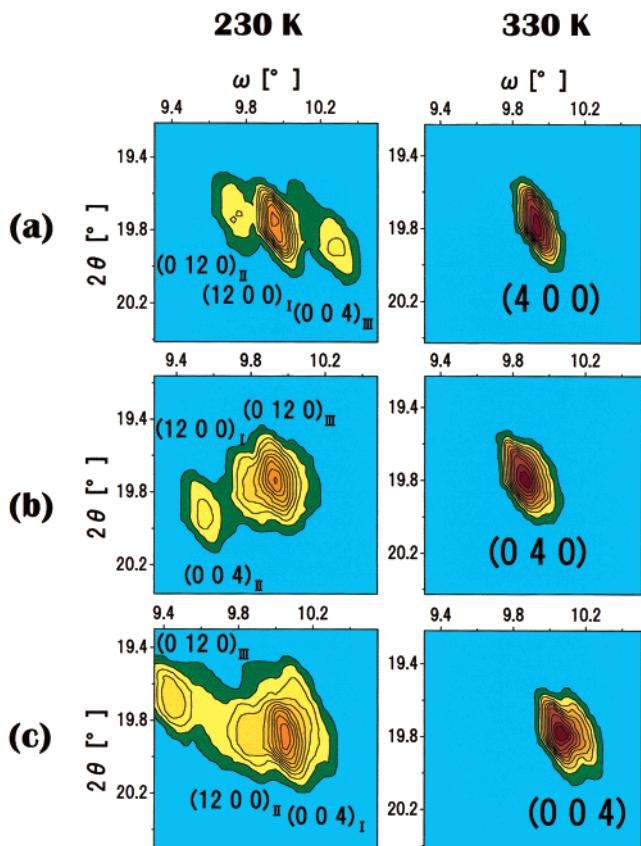
Figure 2. Single-crystal X-ray diffraction reciprocal space mapping of LiMn$_2$O$_4$ around the cubic (a) (4 0 0), (b) (0 4 0) and (c) (0 0 4) reflections at 230 K (left) and 330 K (right), respectively. The indices for three twinning components, I, II, and III, are also shown at 230 K.

fraction data.[11] The oxygen occupation was refined to the nominal value within the experimental error.

Temperature dependence of the structure between 230 and 330 K was precisely investigated on the four-circle diffractometer using a nitrogen gas flow cryostat. The temperature was stable to 0.5 K. Single-crystal X-ray diffraction data were measured after equilibrium of the crystal specimen for 30 min at a given tempera-

(17) Hall, S. R., King, G. S. D., Stewart, J. M., Eds. *Xtal3.4 User's Manual.* University of Western Australia: Lamb, Perth, Australia, 1995.

Figure 3. Temperature dependence of the lattice parameters of the LiMn$_2$O$_4$ single crystal from 300 to 230 K.
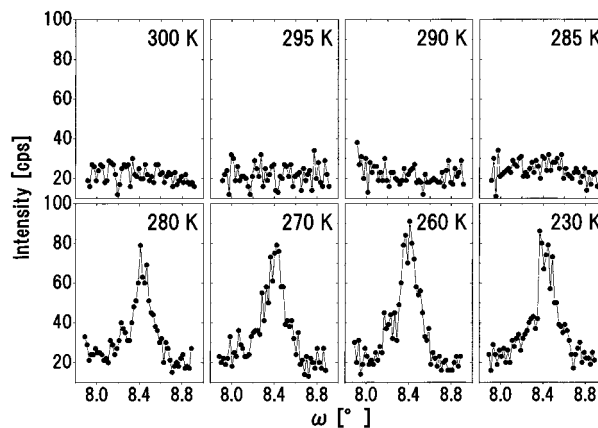
Figure 4. Orthorhombic (2 10 0) superlattice peak profiles at low temperatures. The profiles were examined in the $2\theta-\omega$ scan mode with a step scan interval of 0.02° and a counting time of 2 s.

ture. The structural phase transition at about 285 K on the cooling process has been confirmed by the temperature dependence of peak profiles of the main Bragg reflections.

Single-crystal X-ray diffraction space mapping provides a means of directly observing distortions such as lattice tilting and twinning present in the reciprocal lattice. The value of the lattice parameters directly relates to the peak separation along the 2θ axis, whereas any macroscopic tiltings will show as a difference along the ω axis. We first measured the mapping at 230 K on the four-circle diffractometer and then at 330 K around the same reciprocal lattice points. Shown in Figure 2 are the intensity contour plots for reciprocal space mapping around the cubic (400), (040), (004) reflections at 230 and 330 K, respectively. There are three peaks at 230 K in all these figures with different 2θ and ω values, respectively. On the other hand, there is only one peak at 330 K. From Figure 2, we can clearly see the following.

(i) The crystal is in the orthorhombic symmetry at 230 K. Twins are present in it and the domain ratio for three twinning components, I:II:III, is roughly estimated using the integrated intensity ratio to be 10:2:3. The twin matrix is [0 1 0/0 0 1/1 0 0].

(ii) For the heating process from 230 K, the twinning domains are rearranged together with changing of the lattic parameters, and the good single-crystallinity of

the original cubic spinel structure is recovered above the transition temperature.

Figure 3 presents the temperature dependence of lattice parameters on the cooling process from 300 to 230 K. Because of the differences in the twinning domain ratio of 10:2:3 at low temperatures, the orthorhombic lattice parameters can be determined using the usual peak centering method for 25 well-characterized reflections on the four-circle diffractometer. The hysteresis in the transformation, already observed using powder samples by some researchers, is confirmed by our single-crystal X-ray diffraction study. The evidence of the tripled periodicity has been also found at low temperatures. The orthorhombic (2 10 0) superlattice reflection can be clearly observed below the transition temperature, as shown in Figure 4. Accordingly, the $\sim 3a \times 3a \times a$ orthorhombic lattice parameters were determined to be $a = 24.752(11)$ Å, $b = 24.842(11)$ Å, and $c = 8.209(4)$ Å at 270 K. Further structural properties including a structure refinement of the orthorhombic form using the twinned X-ray intensity data are now being examined.